Chapter 6

Design of Ancillary Controllers for Restructured Electric Market

6.1 Introduction

This chapter presents the application of ancillary services [54, 55, 25] such as power system stabilizers and thyristor control series capacitor in two area deregulated electric market with load frequency control loop. The first order linear model and fourth order model of synchronous machines have been considered for the performance evaluation of the dynamical two area power system. Fourth order model have been considered in the company of automatic voltage regulators. Both the power system stabilizers and thyristor control series capacitor have been simultaneously designed by genetic algorithm and their optimal parameters have been evaluated. The adaptive neuro fuzyy inference system based multiple power system stabilizer and series capacitor have been applied to multiple control area under deregulated electric environment. The distribution participation matrix has been considered according to the various correlative conditions of generating companies and distribution companies. To reflect the effectiveness of power system stabilizers and thyristor control series capacitor in two area of deregulated system, eigen value analysis and non-linear simulation have been performed using linear and non linear model of the synchronous machine respectively.

6.2 Restructured Power System

The traditional two area system of AGC has been modified in restructured electric market [92, 57, 32] to consider the effect of bilateral contracts. The dynamic response of the LFC has been analyzed under effect of bilateral contracts. In deregulated market, DISCO participation factor matrix (DPM) is introduced, which shows different contracts between GENCOs and DISCOs in the two area control loop. DPM consists $n \times m$ matrix, where n is the number of GENCOs and m is the number of DISCOs in control area. DPM is composed of contract participation factor (cpf); cpf_{ij} corresponds to the fraction of the total load power contacted by DISCO j from GENCO i. Figure 6.1 shows schematic diagram of two GENCOs and two DISCOs in each area, according to that, the DPM is described by equation (6.1). The two area interconnected system with TCSC in series with tie line has been shown in Figure 6.2.

$$DPM = \begin{bmatrix} cpf_{11} & cpf_{12} & cpf_{13} & cpf_{14} \\ cpf_{21} & cpf_{22} & cpf_{23} & cpf_{24} \\ cpf_{31} & cpf_{32} & cpf_{33} & cpf_{34} \\ cpf_{41} & cpf_{42} & cpf_{43} & cpf_{44} \end{bmatrix} \tag{6.1}$$

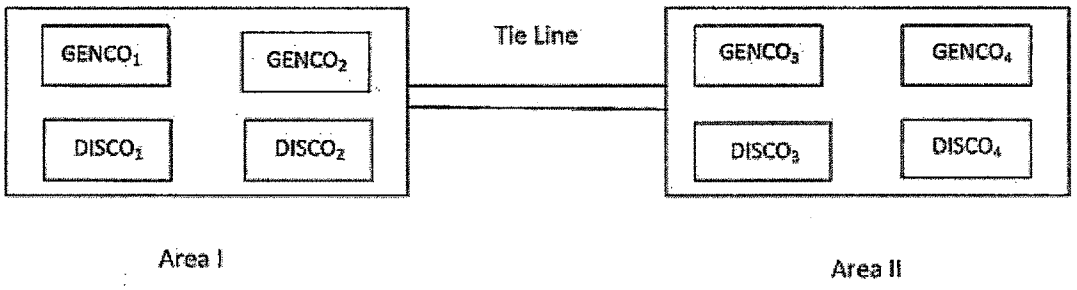

Figure 6.1: Schematic Diagram of Two area system in Restructured Market

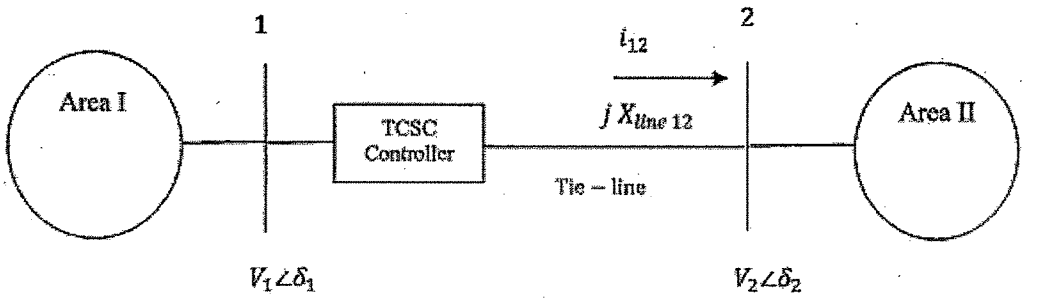

Figure 6.2: Restructured System with TCSC in Series with Tie-Line

Many GENCOs in each area so area control error (ACE) has been distributed among GENCOs. The coefficients that distribute ACE to several GENCOs are called ACE participation factors. According to their participation in the AGC, the ACE participation factors (apfs) distributes ACE to several GENCOs. In deregulated market, a DISCO prefers a particular GENCO for load flow. The scheduled steady state power flow on the tie-line can be given as

$\Delta P_{tie12}^{scheduled}$ = (Demand of DISCOs in area 2 from GENCOs in area 1)-(Demand of DISCOs in aera 1 from GENCOs in area 2)

i.e.

$$\Delta P_{tie12}^{scheduled} = cpf_{12}\Delta P_{L2} - cpf_{21}\Delta P_{L1} \tag{6.2}$$

The tie line power error at any time is defined as :

$$\Delta P_{tie12}^{error} = \Delta P_{tie12}^{actual} - \Delta P_{tie12}^{scheduled} \tag{6.3}$$

When steady state is reached, ΔP_{tie12}^{error} vanishes.

In the AGC scheme, contracted load is forward through the DPM matrix to GENCO set points. The actual load affects system dynamics via the input $\Delta P_{L,LOC}$ to the blocks of the power system. The difference between actual and contracted load demands may results in a frequency deviation that will drive AGC to redispatch GENCOs according to ACE participation factors.

The ACE provides steady state response under normal conditions, but system performance gets affected under the dynamic environment of power system only with ACE in multiarea AGC. Therefore multiple PSS have been suggested with LFC loop. Moreover, in the restructured electric market, various kinds of large capacity equipments and fast power consumption can cause serious problem of frequency oscillation. If system has been not provided with adequate damping, then the oscillation of system frequency may sustain and grow hence, resulting in serious stability problem. The TCSC may be used as a new ancillary service for the stabilization of frequency oscillation of an interconnected thermal power system.

6.3 Design of TCSC Controller with First Order Power System Model

In this section, frequency deviation in two area restructured power system has been analyzed with TCSC controller. The TCSC controller has been used for controlling of tie-line power exchange between two area. The parameters of TCSC controller has been tuned using genetic algorithm. The ANFIS based TCSC controller has been designed from GA based controller. The first order model of power system with turbine and governor system are considered for linear analysis of the two area system. The eigen values analysis have been carried out for stability verification of two area AGC with FACTS controller. The simulation has been performed for analysis of frequency deviation and tie line power in each area with intelligent control techniques under consideration of different DPM. The load frequency controller has controlled the control valves associated with turbine at load variations [15]. Here it is assumed that small variations of load permit the linerization of system equations. The governor and turbine of the system is represented by first order transfer function. The power system is represented by first order model. Here the generator model considered in the present study are described below:

6.3.1 Power system model

The power system loads are composite of a variety of electrical devices. The frequency dependent characteristics of a composite load can be expressed as

$$\Delta P_e = \Delta P_L + D\Delta\omega_m \tag{6.4}$$

where ΔP_L =non frequency sensitive load change, $D\Delta\omega_m$ =frequency sensitive load change, D =load damping constant.

The damping constant is expressed as a percentage change in load for one percent change in frequency. The power system block diagram including the effect of the load damping is shown in Figure 6.3.

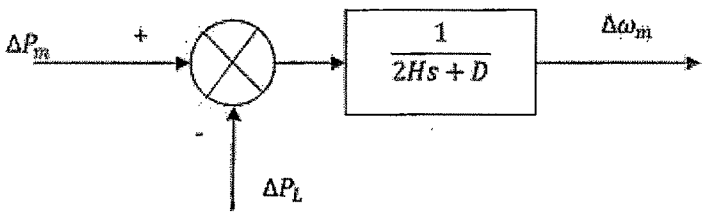

Figure 6.3: First Order Power System

6.3.2 Tie Line Power Flow Model With TCSC

Figure 6.2 shows the schematic diagram of two area interconnected thermal system with TCSC in series with the tie-line. Therefore real power flow can be controlled to mitigate the frequency oscillation and enhance power system stability. Without TCSC, the incrematnal tie line power flow from area 1 to area 2 under open market system can be expressed as equation

$$\Delta P_{tie12}(s) = \frac{2\pi T_{12}}{s}(\Delta F_1(s) - \Delta F_2(s)) \tag{6.5}$$

where T_{12} is the synchronising constant without TCSC.

When TCSC has been placed in series with the tie line as shown in Figure (6.2), the line resistance is to be zero. Current flowing from area 1 to area 2 is i_{12} and power flow equation can be written as follow:

$$P_{tie12} = \frac{|V_1||V_2| sin(\delta_1 - \delta_2)}{X_{net}} \tag{6.6}$$

where X_{net}= X_{line12}−X_{TCSC}

Linearising equation (6.6) using $\Delta X_{net} = -\Delta X_{TCSC}$, equation (6.7) can be obtained. In equation (6.6) perturbing δ_1,δ_2 from their nominal values δ_1^0, δ_2^0 respectively, then

$$\Delta P_{tie12} = \frac{|V_1||V_2|}{X_{net^0}} cos(\delta_1^0 - \delta_2^0) sin(\Delta\delta_1 - \Delta\delta_2) + \frac{|V_1||V_2|}{X_{net^0}^2} sin(\delta_1^0 - \delta_2^0)\Delta X_{TCSC} \tag{6.7}$$

But for a small change in real power load, the variation of bus volatge angles is very small. Therefore $sin(\Delta\delta_1 - \Delta\delta_2) \approx (\Delta\delta_1 - \Delta\delta_2)$, so equation (6.7) is written as

$$\Delta P_{tie12} = \frac{|V_1||V_2|}{X_{net^0}} cos(\delta_1^0 - \delta_2^0)(\Delta\delta_1 - \Delta\delta_2) + \frac{|V_1||V_2|}{X_{net^0}^2} sin(\delta_1^0 - \delta_2^0)\Delta X_{TCSC} \tag{6.8}$$

Above equation is organized as follow:

$$\Delta P_{tie12} = T_{12}(\Delta\delta_1 - \Delta\delta_2) + K_{p1}\Delta X_{TCSC} \tag{6.9}$$

where $T_{12} = \frac{|V_1||V_2|}{X_{net^0}} cos(\delta_1^0 - \delta_2^0)(\Delta\delta_1 - \Delta\delta_2)$ and $K_{p1} = \frac{|V_1||V_2|}{X_{net^0}^2} sin(\delta_1^0 - \delta_2^0)$, so tie line power can be controlled by ΔX_{TCSC}.

But

$$\Delta\delta 1 = 2\pi \int \Delta f_1 dt \tag{6.10}$$

and

$$\Delta\delta 1 = 2\pi \int \Delta f_1 dt \tag{6.11}$$

Equation (6.9) is modified

$$\Delta P_{tie12} = T_{12}(2\pi \int \Delta f_1 dt - 2\pi \int \Delta f_1 dt) + K_{p1}\Delta X_{TCSC} \tag{6.12}$$

Laplace transform of equation (6.12)

$$\Delta P_{tie12} = \frac{2\pi T_{12}}{s}(\Delta F_1(s) - \Delta F_2(s)) + K_{p1}\Delta X_{TCSC} \tag{6.13}$$

As per equation (6.13), it can be observed that the tie line power can be controlled by line reactance. The stability loop of TCSC controller has been used for controlling the tie line power. The ΔX_{TCSC} can be represented by

$$\Delta X_{TCSC}(s) = \frac{K_C T_{W1} s}{1 + T_{W1} s}\left[\frac{(1 + T_{1T}s)(1 + T_{2T}s)}{(1 + T_{3T}s)(1 + T_{4T}s)}\right]\Delta Error(s) \tag{6.14}$$

If speed deviation $\Delta\omega_{m1}$ is sensed, it can be used as control signal, so $\Delta Error = \Delta\omega_{m1}$ to TCSC unit to control ΔX_{TCSC}, which will change tie line power flow between two area and assist in stabilizing the frequency oscillations, Thus

Thus equation (6.13) can be written

$$\Delta P_{tie12} = \frac{2\pi T_{12}}{s}(\Delta F_1(s) - \Delta F_2(s)) + K_{p1}\frac{K_C T_{w1} s}{1 + T_{w1} s}\left[\frac{(1 + T_{1T}s)(1 + T_{2T}s)}{(1 + T_{3T}s)(1 + T_{4T}s)}\right]\Delta\omega_1 \tag{6.15}$$

$$\Delta P_{tie12} = \frac{T_{12}}{s}(\Delta\omega m_1(s) - \Delta\omega_{m2}(s)) + K_{TCSC}\frac{T_{w1} s}{1 + T_{w1} s}\left[\frac{(1 + T_{1T}s)(1 + T_{2T}s)}{(1 + T_{3T}s)(1 + T_{4T}s)}\right]\Delta\omega_1 \tag{6.16}$$

where $K_{TCSC} = K_C K_{p1}$

But in the restructured market system the actual tie line power flow also includes the demand from DISCOs in one area to GENCOs in another area. It can be represented as

$\Delta P_{tie12,actual}$ = $\Delta P_{tie12}(s)$+(demand of DISCOS in area 2 from GENCOS in area 1)-(demand of DISCOS in area 1 from GENCOS in area 2).

6.3.3 Block Diagram and Model of Interconnected Two area System

Figure 6.4 represents block diagram of intelligent controller based TCSC in two area power system under restructured market. Figure 6.4 shows the transfer functions of power system, governor and turbine system with ACE and regulator system in two area AGC under open market scenario. The closed loop system in Figure 6.4 is characterized in state space form as

$\dot{x} = A^{decl}x + B^{decl}u$. The two area system is represented by 16×16 matrix with inclusion of TCSC. The state diagram of TCSC as shown in Figure 2.10 has been used for consideration of modeling for two area system with TCSC controller.

where x is the state vector and u is the vector of power demands of the DISCOs. A^{decl} and B^{decl} are developed from Figure 6.4. The A^{decl} is also defined as stability matrix. The eigen values of the system can be calculated using stability matrix. The eigen values shows the position of closed loop poles in s-palne, through these values effectiveness of TCSC in AGC system can be verified. A^{decl} and B^{decl} are represented by equation (6.17) and (6.18) respectively. The state matrix x of variables and input matrix u are mention.

$$A^{decl} = \begin{bmatrix} A_1 & A_2 \\ A_3 & A_4 \end{bmatrix}_{16\times16} \tag{6.17}$$

Where,

$$A_1 = \begin{bmatrix} -\frac{1}{Tp_1} & 0 & \frac{Kp_1}{Tp_1} & \frac{Kp_1}{Tp_1} & 0 & 0 & 0 & 0 \\ 0 & -\frac{1}{Tp_2} & 0 & 0 & \frac{Kp_1}{Tp_2} & \frac{Kp_2}{Tp_2} & 0 & 0 \\ 0 & 0 & -\frac{1}{Tt_1} & 0 & 0 & 0 & -\frac{1}{Tt_1} & 0 \\ 0 & 0 & 0 & -\frac{1}{Tt2_2} & 0 & 0 & 0 & -\frac{1}{Tt_2} \\ 0 & 0 & 0 & 0 & \frac{1}{-Tt_3} & 0 & 0 & 0 \\ 0 & 0 & 0 & 0 & 0 & \frac{1}{-Tt_4} & 0 & 0 \\ -\frac{1}{2\pi R_1 Tg_1} & 0 & 0 & 0 & 0 & 0 & -\frac{1}{Tg_1} & 0 \\ -\frac{1}{2\pi R_1 Tg_2} & 0 & 0 & 0 & 0 & 0 & 0 & -\frac{1}{Tg_2} \end{bmatrix}$$

$$A_2 = \begin{bmatrix} 0 & 0 & 0 & 0 & 0 & 0 & -\frac{Kp_1}{Tp_1} & -\frac{Kp_1}{Tp_1} \\ 0 & 0 & 0 & 0 & 0 & 0 & -\frac{a_{12}K_{p1}}{Tp1} & -\frac{a_{12}K_{p1}}{Tp_2} \\ 0 & 0 & 0 & 0 & 0 & 0 & 0 & 0 \\ 0 & 0 & 0 & 0 & 0 & 0 & 0 & 0 \\ -\frac{1}{Tt_3} & 0 & 0 & 0 & 0 & 0 & 0 & 0 \\ 0 & -\frac{1}{Tt_4} & 0 & 0 & 0 & 0 & 0 & 0 \\ 0 & 0 & -\frac{K_1 apf_1}{Tg_1} & 0 & 0 & 0 & 0 & 0 \\ 0 & 0 & -\frac{K_1 apf_2}{Tg_2} & 0 & 0 & 0 & 0 & 0 \end{bmatrix}$$

$$A_3 = \begin{bmatrix} 0 & -\frac{1}{2\pi R_1 Tg_3} & 0 & 0 & 0 & 0 & 0 & 0 \\ 0 & -\frac{1}{2\pi R_1 Tg_4} & 0 & 0 & 0 & 0 & 0 & 0 \\ \frac{B_1}{2\pi} & 0 & 0 & 0 & 0 & 0 & 0 & 0 \\ 0 & \frac{B_2}{2\pi} & 0 & 0 & 0 & 0 & 0 & 0 \\ \frac{-Kc}{Tp1} & 0 & \frac{Kp_1Kc}{Tp1} & \frac{Kp_1Kc}{Tp1} & 0 & 0 & 0 & 0 \\ \frac{(KcT_{1T})}{T_{2T}Tp_1} & 0 & \frac{T_{1T}Kp_1Kc}{T_{2T}Tp_1} & \frac{T_{1T}Kp_1Kc}{T_{2T}Tp1} & 0 & 0 & 0 & 0 \\ a & 0 & b & c & 0 & 0 & 0 & 0 \\ \frac{T12}{2\pi} & -\frac{T12}{2\pi} & 0 & 0 & 0 & 0 & 0 & 0 \end{bmatrix}$$

$$A_4 = \begin{bmatrix} -\frac{1}{Tg_3} & 0 & 0 & -\frac{K_2apf_3}{Tg_3} & 0 & 0 & 0 & 0 \\ 0 & -\frac{1}{Tg_4} & 0 & -\frac{K_2apf_4}{Tg_4} & 0 & 0 & 0 & 0 \\ 0 & 0 & 0 & 0 & 1 & 0 & 0 & 0 \\ 0 & 0 & 0 & 0 & -1 & 0 & 0 & 0 \\ 0 & 0 & 0 & 0 & -\frac{1}{Tw} & 0 & 0 & -\frac{Kp1Kc}{Tp1} \\ 0 & 0 & 0 & 0 & \frac{1/T_{2T}-T_{1T}}{T_{2T}Tw} & \frac{1}{T2T} & 0 & \frac{Kp_1KcT_{1T}}{Tp_1T_{2T}} \\ 0 & 0 & 0 & 0 & m & n & -\frac{1}{4T} & p \\ 0 & 0 & 0 & 0 & 0 & 0 & 1 & 0 \end{bmatrix}$$

Where,

$a = -\frac{KcT_{1T}T_{3T}}{T_{2T}Tp_1T_{4T}}, b = \frac{T_{1T}Kp_1KcT_{3T}}{T_{2T}Tp_1T_{4T}}, c = \frac{KcKp_1T_{1T}T3}{T_{4T}Tp1T2T}, m = \frac{T_{3T}/T_{2T}T_{4T}}{T_1T_{T3T}/T_{2T}T_{4T}Tw}, n = \frac{1/T_{4T}}{T_{3T}/(T_{2T}T_{4T})}, p = -\frac{KcT_{3T}T_1TKp_1}{T_{2T}T_{4T}Tp_1}$

$$B^{decl} = \begin{bmatrix} B_1 & B_2 \\ B_3 & B_4 \end{bmatrix}_{16\times 6} \tag{6.18}$$

Where,

$$B_1 = \begin{bmatrix} -\frac{Kp1}{Tp1} & -\frac{Kp1}{Tp1} & 0 \\ 0 & 0 & -\frac{Kp2}{Tp2} \\ 0 & 0 & 0 \\ 0 & 0 & 0 \\ 0 & 0 & 0 \\ 0 & 0 & 0 \\ \frac{cpf_{11}}{Tg_1} & \frac{cpf_{12}}{Tg_1} & \frac{cpf_{13}}{Tg_1} \\ \frac{cpf_{21}}{Tg_2} & \frac{cpf_{21}}{Tg_2} & \frac{cpf_{21}}{Tg_2} \end{bmatrix}$$

$$B_2 = \begin{bmatrix} 0 & -\frac{Kp1}{Tp1} & 0 \\ -\frac{Kp2}{Tp2} & 0 & -\frac{Kp2}{Tp2} \\ 0 & 0 & 0 \\ 0 & 0 & 0 \\ 0 & 0 & 0 \\ 0 & 0 & 0 \\ \frac{cpf_{14}}{Tg_1} & 0 & 0 \\ \frac{cpf_{21}}{Tg_2} & 0 & 0 \end{bmatrix}$$

$$B_3 = \begin{bmatrix} \frac{cpf_{31}}{Tg_3} & \frac{cpf_{31}}{Tg_3} & \frac{cpf_{31}}{Tg_3} \\ \frac{cpf_{41}}{Tg_4} & \frac{cpf_{41}}{Tg_4} & \frac{cpf_{41}}{Tg_4} \\ cpf_{31} + cpf_{41} & cpf_{32} + cpf_{42} & -(cpf_{13} + cpf_{23}) \\ -(cpf_{31} + cpf_{41}) & -(cpf_{32} + cpf_{42}) & cpf_{13} + cpf_{23} \\ 0 & 0 & 0 \\ 0 & 0 & 0 \\ 0 & 0 & 0 \\ 0 & 0 & 0 \end{bmatrix}$$

$$B_4 = \begin{bmatrix} \frac{cpf_{31}}{Tg_3} & 0 & 0 \\ \frac{cpf_{41}}{Tg_4} & 0 & 0 \\ -(cpf_{14} + cpf_{24}) & 0 & 0 \\ cpf_{14} + cpf_{24} & 0 & 0 \\ 0 & 0 & 0 \\ 0 & 0 & 0 \\ 0 & 0 & 0 \\ 0 & 0 & 0 \end{bmatrix}$$

Where,

$$x = \begin{bmatrix} \Delta\omega_1 & \Delta\omega_2 & \Delta P_{GV1} & \Delta P_{GV2} & \Delta P_{GV3} & \Delta P_{GV4} & \Delta P_{M1} & \Delta P_{M2} \end{bmatrix}' \text{ Contd...}$$

$$x = \begin{bmatrix} \Delta P_{M3} & \Delta P_{M4} & \int ACE_1 dt & \int ACE_1 dt & \Delta X_1 & \Delta X_2 & \Delta X_{TCSC} & \Delta P_{tie1-2} \end{bmatrix}'_{16\times1}$$

$$u = \begin{bmatrix} \Delta P_{L1} & \Delta P_{L1} & \Delta P_{L3} & \Delta P_{L4} & \Delta P_{L1,LOC} & \Delta P_{L2,LOC} \end{bmatrix}'_{6\times1}$$

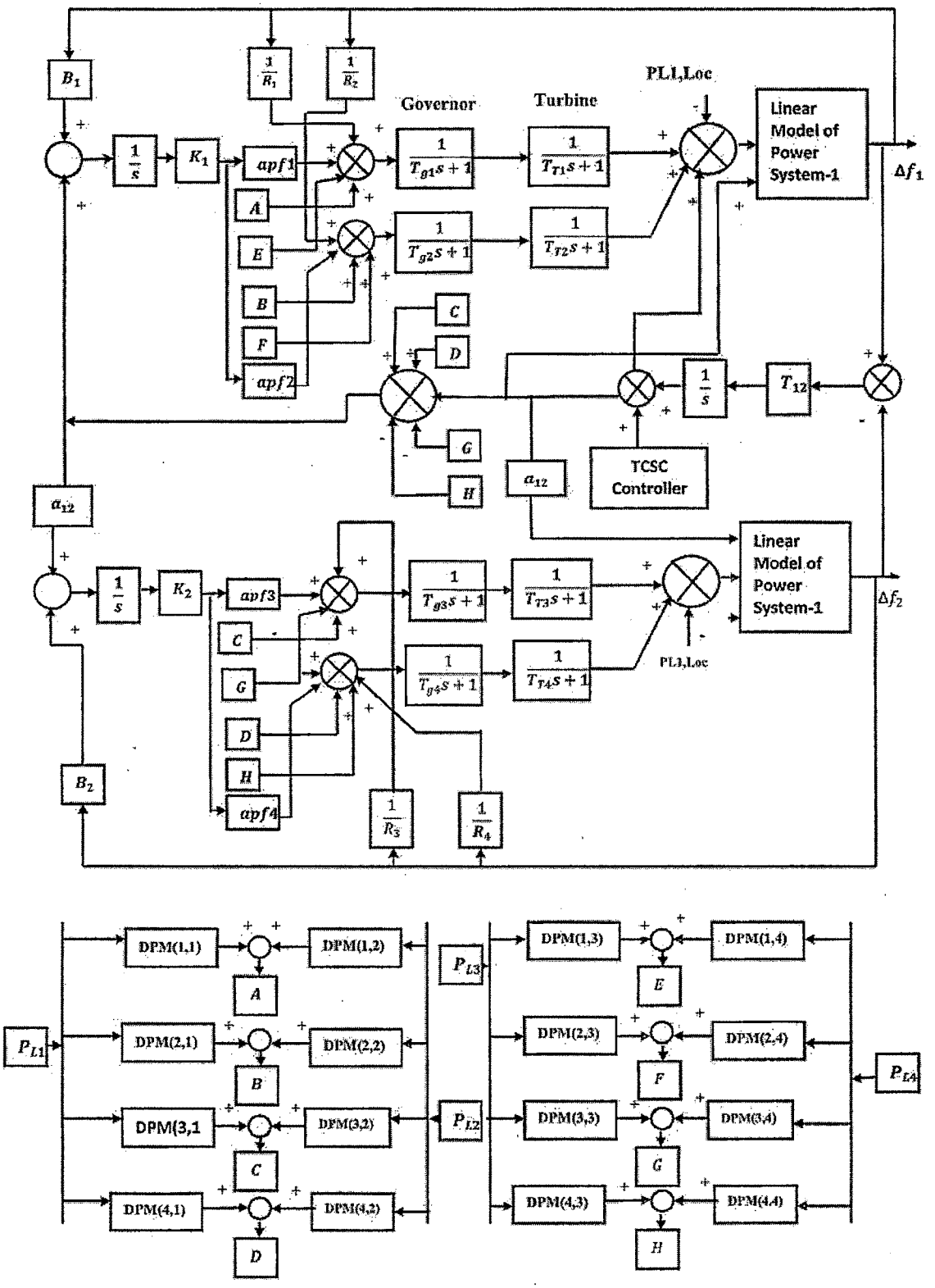

Figure 6.4: Intelligent techniques based TCSC for two area system under restructured market

6.3.4 GA- tie line TCSC Controller: Problem Formulation and Optimization Function

The stability loop equation (2.89) has been used for frequency stabilization. The input signal rotor speed deviation of area 1 or area 2 has been chosen for TCSC proposed controller. The equation (6.16) consists wash out filter time constant T_{w1}, gain K_{TCSC} and time constant of phase compensator T_{1T}, T_{2T}, T_{3T} and T_{4T}, which provides appropriate phase-lead characteristics to compensate for the phase lag between input and output signals. Thus, five parameters such as gain K_{TCSC} and time constant parameter $T_{1T}, T_{2T}, T_{3T}, T_{4T}$ are required to be optimized for the optimal design of TCSC frequency controller. For TCSC, the time constant of wash out filter T_{w1} has been selected to be 10. The objective of LFC with tie line TCSC controller is, to reduce the oscillatory frequency in rotor mode and to minimize the tie line power oscillation in both control area. The goal can be achieved after minimizing the optimization function J, which is described by equation (6.19). The optimization function has been developed such that the damping factor of rotor mode in LFC be improved and minimization of real part of the eigen values associated with the rotor mode. Hence time response parameters such as settling time to be improved and overshoots to be reduced. The Time Multiplied by Absolute Error (ITAE) has been used as the performance index. The optimization function J follows the optimized performance of TCSC controlled system. The gains for the TCSC controller are adjusted such that the performance index be minimized. The performance index is calculated over a time interval T, normally in the region of, where t is the settling time of the system. The best system response is obtained when the tie line power controller TCSC parameters are optimized by minimizing the maximum eigen values over a certain range of operating conditions. The optimization flow chart for implementation of real coded GA is similar as shown in Figure 3.3. However, here only TCSC tie line controller parameters are required to be optimized as described by equations (6.20) to (6.24). The optimization function J is as follows :

$$J = \int_0^T t\,|\triangle\omega_{m1}(t)|\,dt \tag{6.19}$$

with

$$T_{1T}^{min} \leq T_{1T} \leq T_{1T}^{max} \tag{6.20}$$

$$T_{2T}^{min} \leq T_{2T} \leq T_{2T}^{max} \tag{6.21}$$

$$T_{3T}^{min} \leq T_{3T} \leq T_{4T}^{max} \tag{6.22}$$

$$T_{4T}^{min} \leq T_{4T} \leq T_{4T}^{max} \tag{6.23}$$

$$K_{TCSC}^{min} \leq K_{TCSC} \leq K_{TCSC}^{max} \tag{6.24}$$

6.3.5 ANFIS- Tie Line TCSC Controller

Here, GA-TCSC is replaced by the ANFIS based TCSC. The mathematical model of the two area LFC system with GA-TCSC as shown in Figure 6.4 has been used for the generation of the training data pair for the ANFIS-TCSC. The Takagi-Sugeno FIS is used for the design of ANFIS based TCSC. The ANFIS architecture and algorithm steps described by section (4.2) and section (4.3) have been implemented for designing of ANFIS based tie line TCSC respectively. The network has been trained using 1000 sample data, which are generated under the consideration of the different correlative conditions between GENCOs and DISCOs and different values of six inputs of the system. The two inputs and one output have been used for the training of ANFIS. The dynamic inputs are speed $\Delta\omega_{m1}(t)$ and change in speed $(\frac{\Delta d\omega_{m1}(t)}{dt})$, and corresponding ΔX_{TCSC} has been selected as output value of the ANFIS.

6.3.6 Simulation and Results

The model presented by Figure 6.4 has been used for stability analysis of the two area system with TCSC. The eigen values, damping factors and participation factors of the system are calculated using MATLAB programming. The objective function described by equations (6.20) to (6.24) have been optimized. The time domain simulation is performed and fitness value is determined through equation (6.19) for gain and time constant parameters of TCSC. By changing the GA parameters such as population size, crossover rate and function, mutation rate and function, number of generation, etc, the new set of gains and time constants have been developed and best fitness values have been selected. The optimized parameters of TCSC are tuned for expected solution which is given by Table 6.2. eigen values and damping factor without application of TCSC and with application of TCSC have been shown in Table 6.1.

Table 6.1: Eigen values without TCSC and with TCSC

without TCSC			with TCSC	
	eigen values	ζ	eigen values	ζ
area 1	0.2312 + 1.9285i	-0.1191	-0.0361 + 5.4791i	0.0066
	0.2312 - 1.9285i	-0.1191	-0.0361 - 5.4791i	0.0066
area 2	-0.5908 + 0.7397i	0.6241	-0.3780 + 0.9571i	0.3673
	-0.5908 - 0.7397i	0.6241	-0.3780 - 0.9571i	0.3673

Table 6.2: Optimized Parameters of TCSC

Parameters	Values
K_{TCSC}	5.252
T_{1T}	0.01382
T_{2T}	0.01091
T_{3T}	0.01135
T_{4T}	0.01645

Attention to Table 6.1, Without TCSC, the eigen value associated with area 1 is positive and in area 2 is negative. With TCSC, eigen values and the damping factor associated to rotor mode in two area LFC have been significantly improved. hence, the TCSC tie line

power controller provides good stability to the multiple area power system and closed poles are far away in the left half of the s-pane using TCSC compared to without controller.

Case I:

A two area system is used to demonstrate the behavior of the AGC scheme with TCSC frequency stabilizer. The different cases [32] are considered according to the bilateral contract between GENCOs and DISCOs in restructured market. The comparison analysis between GA based TCSC and ANFIS based TCSC in restructured AGC scheme have been carried out. The data described by Appendix B are used for the simulation purpose. The governor and turbine units in each area assumed to be identical. In this case, the GENCOs in each area participate equally in AGC. ACE participation factors are $apf_1 = 0.5, apf_2 = 0.5, apf_3 = 0.5, apf_4 = 0.5$. Assume that the load change occurs only in area 1. Thus, the load is demanded only by DISCO1 and DISCO2. Load variation in area 1 is $\Delta P_{L1} = 0.05$ p.u., $\Delta P_2 = 0.05$ p.u., $\Delta P_{L1,LOC} = 0.1$p.u. are considered and no disturbances occur in area II. The optimal integral gain $K_1 = 0.9$ and $K_2 = 0.1$ are selected [76] The DPM is described by equation (6.25). Figure 6.5 shows the response of speed deviation without TCSC in both area. The response of speed deviation with GA and ANFIS based TCSC in both area has been shown in Figure 6.6 and 6.7 respectively. Figure 6.8 shows the tie line power oscillation response in both area with TCSC controller.

$$DPM = \begin{bmatrix} 0.50 & 0.50 & 0.00 & 0.00 \\ 0.50 & 0.50 & 0.00 & 0.00 \\ 0.00 & 0.00 & 0.00 & 0.00 \\ 0.00 & 0.00 & 0.00 & 0.00 \end{bmatrix} \tag{6.25}$$

Case II: In this case, where all the DISCOs contract with GENCOs for power as per DPM described by equation (6.26). ACE participation factors are $apf_1 = 0.75, apf_2 = 0.25, apf_3 = 0.5, apf_4 = 0.5$. The load variation are considered such as $\Delta P_{L1} = 0.01$ p.u., $\Delta P_2 = 0.02$ p.u.,$\Delta P_{L3} = -0.05$p.u.,$\Delta P_{L4} = 0.1$p.u.,$\Delta P_{L1,Loc} = -0.1$p.u. and $\Delta P_{L2,Loc} = 0$. Figure 6.9 shows the response of speed deviation without TCSC in both area. The response

of speed deviation with GA and ANFIS based TCSC in both area has been shown in Figure 6.10 and 6.11 respectively. Figure 6.12 shows the tie line power oscillation response in both area with TCSC controller.

$$DPM = \begin{bmatrix} 0.50 & 0.25 & 0.00 & 0.30 \\ 0.20 & 0.25 & 0.00 & 0.00 \\ 0.00 & 0.25 & 1.00 & 0.70 \\ 0.30 & 0.25 & 0.00 & 0.00 \end{bmatrix} \tag{6.26}$$

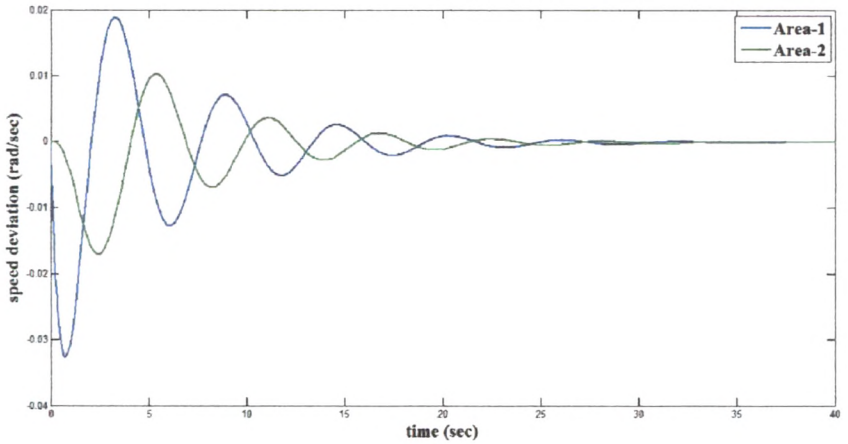

Figure 6.5: Case I: Speed deviation in Restructured Market without Tie Line Controller

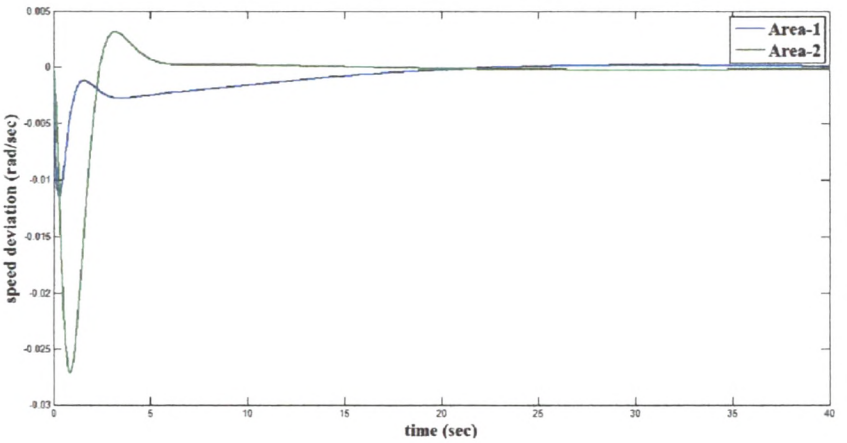

Figure 6.6: Case I: Speed deviation in Restructured Market with GA-TCSC Tie Line controller

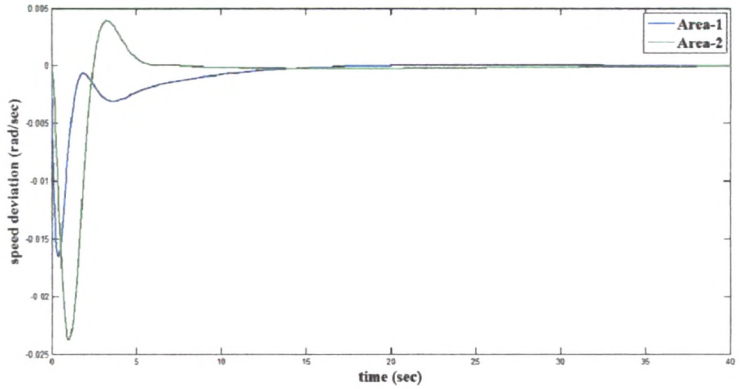

Figure 6.7: Case I: Speed Deviation in Restructured Market with ANFIS-TCSC Tie Line controller

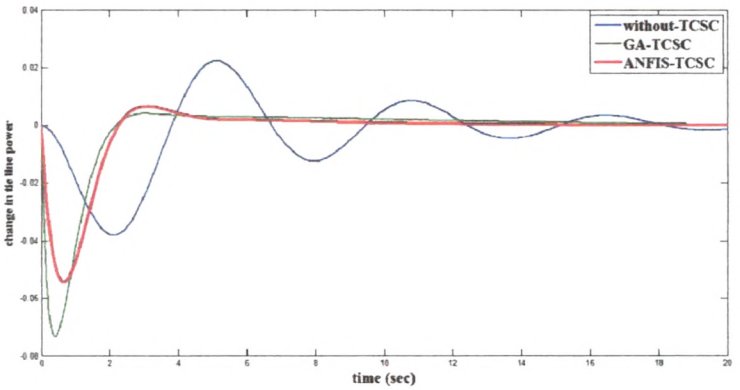

Figure 6.8: Case I: Tie Line Power Change with Controllers

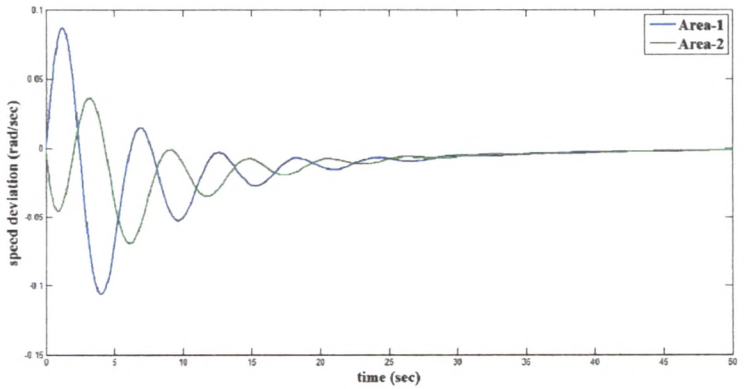

Figure 6.9: Case II: Speed deviation In Restructured Market without Tie Line Controller

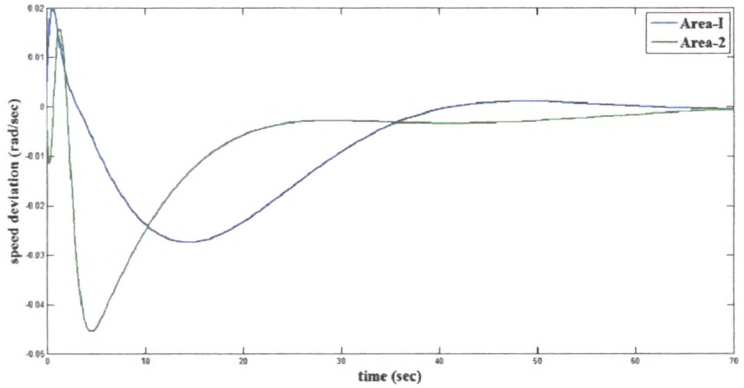

Figure 6.10: Case II: Speed deviation in Restructured Market with GA-TCSC Tie Line Controller

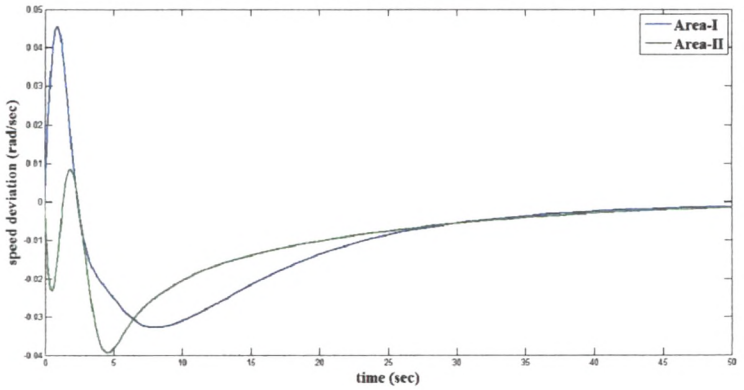

Figure 6.11: Case II : Speed deviation in Restructured Market with ANFIS-TCSC Tie Line Controller

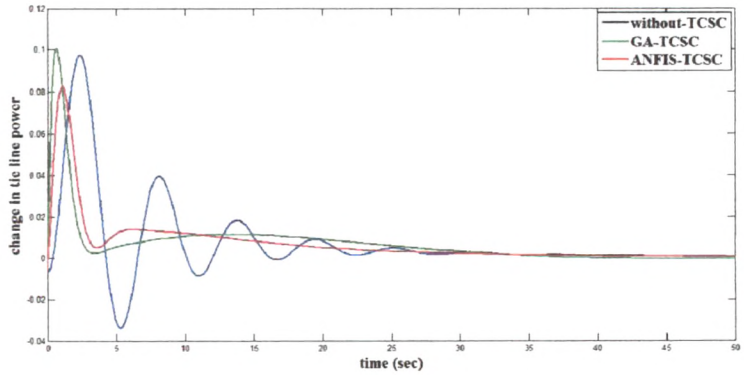

Figure 6.12: Case II: Tie Line Power Change With Controllers

6.3.7 Discussion

Here linear power system model has been used for two area LFC loop in deregulated electric market. The oscillatory frequency in two area have been controlled by tie line TCSC controller with different disturbances and consideration of various DPM. eigen values analysis show that the tie line power controller has provided good stability to the multiarea system. The effect of various DPM and variation of load have been clearly observed in the simulation results of speed deviation and change in tie line power. The simulation results show that the frequency oscillation as shown in Figures 6.6, 6.7, 6.10, 6.11 and tie line power oscillation as shown Figures 6.8 and 6.12 have been controlled through GA and ANFIS based TCSC in two area system. The settling time and overshoot in both control area without TCSC has been given in Table 6.3. Comparison analysis between GA and ANFIS based TCSC have been given in Table 6.4 and 6.5 respectively. In case II, ANFIS based TCSC has performed better than GA tuned TCSC controller. The responses of oscillation in speed deviation and tie line power have been improved using ANFIS-TCSC controller. Here TCSC controller has reduced oscillations significantly in speed deviation as well as tie line power in both area. The settling time of responses have been improved using TCSC tie line controller compared to that without TCSC.

Table 6.3: Time Response Parameters without Tie-Line TCSC Controller

Area		Speed deviation		Tie-line power	
		Settling time(s)	Overshoot(rad/sec)	Settling time(s)	Overshoot(p.u.)
Case I	area-1	38	-0.0327	35	-0.018
	area-2	38	-0.017		
Case II	area-1	50	0.08	45	0.098
	area-2	50	0.025		

Table 6.4: Time Response Parameters with Tie-line GA-TCSC Controller

Area		Speed deviation		Tie-line power	
		Settling time(s)	Overshoot(rad/sec)	Settling time(s)	Overshoot(p.u.)
Case I	area 1I	25	-0.0111	20	-0.072
	area 2	17.5	-0.0273		
Case II	area 1	60	0.02	40	0.1
	area 2	70	-0.045		

Table 6.5: Time Response Parameters with Tie-line ANFIS-TCSC Controller

Area		Speed deviation		Tie-line power	
		Settling time(s)	Overshoot(rad/sec)	Settling time(s)	Overshoot(p.u.)
Case I	area 1	28	-0.0166	16	-0.05
	area 2	28	-0.0238		
Case II	area 1	45	0.045	35	0.08
	area 2	45	-0.04		

However, effect of exciter and power system stabilizer can not be analyzed considering the first order linear model of power system. The non linear simulation and transient analysis can't be performed using same model. So, it is essential to consider higher order linear and non linear model of power system for depth analysis of multiarea power system for verification of role of tie line power controller as well as other supplementary controllers such as PSS.

6.4 Design of PSS and TCSC Controller with Fourth order Power System Model

In this section, frequency deviation in two area restructured power system has been analyzed with multiple PSS and TCSC controller. The parameters of PSS and TCSC controller have been tuned using genetic algorithm. The ANFIS based PSS and TCSC controllers have been designed from GA based controller. The fourth order power system a company of AVR with turbine and governor system have been considered for analysis of the two area system. The

eigen values analysis have been carried out for stability verification of two area AGC with PSS and FACTS controller. The non-linear simulation has been performed for analysis of frequency deviation and tie line power in each area with intelligent control techniques under consideration of different DPM.

6.4.1 Power System Model

6.4.1.1 Model of Power System with multiple PSS

Figure 6.13 represents block diagram of intelligent controller based PSS in two area power system under restructured market. The linear model of power system consists fifth order linear equations with AVR. The block diagram described by Figure 2.3 has been utilized as power system 1 and power system 2 in area control loop. The equation (2.78) of power system stabilizer is included in machine state equations and described in state space form $\Delta\dot{x} = A\Delta x + B\Delta u$. Here one stage phase compensator of PSS with gain and washout filter has been considered. The complete closed loop two area system AGC with PSSs can be represented by 25 × 25 matrix. The closed loop system in Figure 6.13 is characterized in state space form as

$$\dot{x} = A^{declpss}x + B^{declpss}u \tag{6.27}$$

where x is the state vector and u is the vector of power demands of the DISCOs. $A^{declpss}$ and $B^{declpss}$ are developed from Figure 6.13. The $A^{declpss}$ is also defined as stability matrix. The eigen values of the system can be calculated using stability matrix. $A^{declpss}$ is represented by equation (6.28).

6.4.1.2 Model of Power System with PSSs and TCSC

The two area interconnected system with tie line TCSC controller is shown in Figure 6.4. The state diagram of TCSC as shown in Figure 2.10 has been used for consideration of

modeling for two area system with TCSC controller. The complete closed loop two area system with TCSC can be represented by 24×24 matrix. Figure 6.13 has been modified with effect of TCSC controller and mathematical model of simultaneous application of TCSC and PSSs can be described by 28×28 matrix.

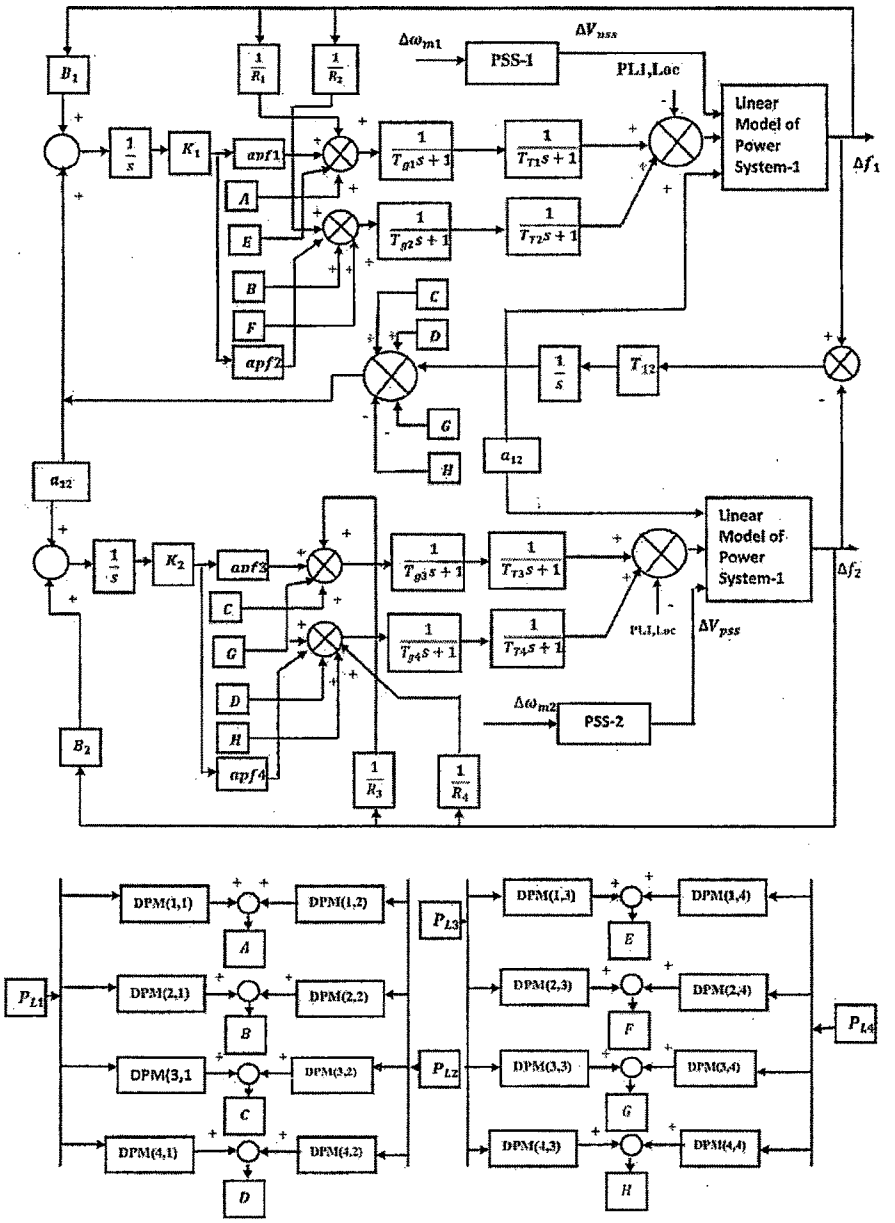

Figure 6.13: Two area interconnection system with multiple PSS in restructured market

$$A^{declpss} = \begin{bmatrix}
\frac{-D}{2H} & 0 & \frac{-K_1}{2H} & 0 & \frac{-K_2}{2H} & 0 \\
0 & -\frac{D}{2H} & 0 & -\frac{K_1}{2H} & 0 & \frac{-K_2}{2H} \\
wb & 0 & 0 & 0 & 0 & 0 \\
0 & wb & 0 & 0 & 0 & 0 \\
0 & 0 & -\frac{K_5}{T'_{d0}} & 0 & -\frac{1}{K_4 T'_{d0}} & 0 \\
0 & 0 & 0 & -\frac{K_5}{T'_{d0}} & 0 & -\frac{1}{K_4 T'_{d0}} \\
0 & 0 & -\frac{K_7}{T'_{q0}} & 0 & 0 & -\frac{1}{K_6 T'_{q0}} \\
0 & 0 & 0 & -\frac{K_7}{T'_{q0}} & 0 & 0 \\
0 & 0 & -\frac{K_A K_8}{T_A} & 0 & -\frac{K_A K_9}{T_A} & 0 \\
0 & 0 & 0 & -\frac{K_A K_8}{T_A} & 0 & -\frac{K_A K_9}{T_A} \\
0 & 0 & 0 & 0 & 0 & 0 \\
0 & 0 & 0 & 0 & 0 & 0 \\
0 & 0 & 0 & 0 & 0 & 0 \\
0 & 0 & 0 & 0 & 0 & 0 \\
-\frac{1}{2\pi R_1 T_{G1}} & 0 & 0 & 0 & 0 & 0 \\
-\frac{1}{2\pi R_2 T_{G2}} & 0 & 0 & 0 & 0 & 0 \\
0 & -\frac{1}{2\pi R_3 T_{G3}} & 0 & 0 & 0 & 0 \\
0 & -\frac{1}{2\pi R_4 T_{G4}} & 0 & 0 & 0 & 0 \\
\frac{B1}{2\pi} & 0 & 0 & 0 & 0 & 0 \\
0 & \frac{B1}{2\pi} & 0 & 0 & 0 & 0 \\
\frac{T_{12}}{2\pi} & -\frac{T_{12}}{2\pi} & 0 & 0 & 0 & 0 \\
-\frac{K_{pss} D}{2H} & 0 & -\frac{K_1 K_{pss}}{2H} & 0 & -\frac{K_2 K_{pss}}{2H} & 0 \\
-\frac{K_{pss} D T_1}{T_2 2H} & 0 & -\frac{K_{pss} K_1 T_1}{T_2 2H} & 0 & -\frac{K_2 K_{pss} T_1}{2H T_2} & 0 \\
0 & a3 & 0 & b3 & 0 & c3 \\
0 & a4 & 0 & b4 & 0 & c4
\end{bmatrix}$$

Contd....

$$
\begin{bmatrix}
\frac{-K_3}{2H} & 0 & 0 & 0 & \frac{1}{2H} & \frac{1}{2H} & 0 & 0 & 0 & 0 \\
0 & \frac{-K_3}{2H} & 0 & 0 & 0 & 0 & \frac{1}{2H} & \frac{1}{2H} & 0 & 0 \\
0 & 0 & 0 & 0 & 0 & 0 & 0 & 0 & 0 & 0 \\
0 & 0 & 0 & 0 & 0 & 0 & 0 & 0 & 0 & 0 \\
0 & 0 & \frac{1}{T'_{d0}} & 0 & 0 & 0 & 0 & 0 & 0 & 0 \\
0 & 0 & 0 & \frac{1}{T'_{d0}} & 0 & 0 & 0 & 0 & 0 & 0 \\
0 & 0 & 0 & 0 & 0 & 0 & 0 & 0 & 0 & 0 \\
0 & -\frac{1}{K_6 T'_{q0}} & 0 & 0 & 0 & 0 & 0 & 0 & 0 & 0 \\
-\frac{K_A K_{10}}{T_A} & 0 & -\frac{1}{T_A} & 0 & 0 & 0 & 0 & 0 & 0 & 0 \\
0 & -\frac{K_A K_{10}}{T_A} & 0 & -\frac{1}{T_A} & 0 & 0 & 0 & 0 & 0 & 0 \\
0 & 0 & 0 & 0 & -\frac{1}{T_{T1}} & 0 & 0 & 0 & \frac{1}{T_{T2}} & 0 \\
0 & 0 & 0 & 0 & 0 & -\frac{1}{T_{T2}} & 0 & 0 & 0 & \frac{1}{T_{T2}} \\
0 & 0 & 0 & 0 & 0 & 0 & -\frac{1}{T_{T3}} & 0 & 0 & 0 \\
0 & 0 & 0 & 0 & 0 & 0 & 0 & -\frac{1}{T_{T4}} & 0 & 0 \\
0 & 0 & 0 & 0 & 0 & 0 & 0 & 0 & -\frac{1}{T_{G2}} & 0 \\
0 & 0 & 0 & 0 & 0 & 0 & 0 & 0 & 0 & -\frac{1}{T_{G2}} \\
0 & 0 & 0 & 0 & 0 & 0 & 0 & 0 & 0 & 0 \\
0 & 0 & 0 & 0 & 0 & 0 & 0 & 0 & 0 & 0 \\
0 & 0 & 0 & 0 & 0 & 0 & 0 & 0 & 0 & 0 \\
0 & 0 & 0 & 0 & 0 & 0 & 0 & 0 & 0 & 0 \\
0 & 0 & 0 & 0 & 0 & 0 & 0 & 0 & 0 & 0 \\
-\frac{K_3 K_{pss}}{2H} & 0 & 0 & 0 & \frac{K_{pss}}{2H} & \frac{K_{pss}}{2H} & 0 & 0 & 0 & 0 \\
-\frac{K_3 K_{pss} T_1}{T_2 2H} & 0 & 0 & 0 & \frac{K_{pss} T_1}{T_2 2H} & \frac{K_{pss} T_1}{T_2 2H} & 0 & 0 & 0 & 0 \\
0 & d3 & 0 & 0 & 0 & 0 & e3 & f3 & 0 & 0 \\
0 & d4 & 0 & 0 & 0 & 0 & e4 & f4 & 0 & 0
\end{bmatrix}
$$

Contd...

Where,

$a3 = -DK_{pss1}/2H, b3 = -K_1 K_{pss1}/2H, c3 = -K_2 K_{pss1}/2H, d3 = -K_3 K_{pss1}/2H,$

$e3 = K_{pss1}/2H, f3 = K_{pss1}/2H, g3 = -a_{12} K_{pss1}/2H, h3 = -1/T_w$

$a4 = -DK_{pss2} T_1/2HT_2, b4 = -K_{pss2} K_1 T_1/2HT_2, c4 = -K_{pss2} K_2 T_1/2HT_2,$

$d4 = -K_{pss2} K_3 T_1/2HT_2, e4 = -K_{pss2} T_1/2HT_2, f4 = -K_{pss2} T_1/2HT_2,$

$g4 = -K_{pss2}T_1a_{12}/2HT_2, h4 = (1/T_2) - T_1/(T_2T_w)$

$$\begin{bmatrix}
0 & 0 & 0 & 0 & \frac{-1}{2H} & 0 & 0 & 0 & 0 \\
0 & 0 & 0 & 0 & \frac{-1}{2H} & 0 & 0 & 0 & 0 \\
0 & 0 & 0 & 0 & 0 & 0 & 0 & 0 & 0 \\
0 & 0 & 0 & 0 & 0 & 0 & 0 & 0 & 0 \\
0 & 0 & 0 & 0 & 0 & 0 & 0 & 0 & 0 \\
0 & 0 & 0 & 0 & 0 & 0 & 0 & 0 & 0 \\
0 & 0 & 0 & 0 & 0 & 0 & 0 & 0 & 0 \\
0 & 0 & 0 & 0 & 0 & 0 & 0 & 0 & 0 \\
0 & 0 & 0 & 0 & 0 & 0 & \frac{K_A}{T_A} & 0 & 0 \\
0 & 0 & 0 & 0 & 0 & 0 & 0 & 0 & \frac{K_A}{T_A} \\
0 & 0 & 0 & 0 & 0 & 0 & 0 & 0 & 0 \\
0 & 0 & 0 & 0 & 0 & 0 & 0 & 0 & 0 \\
\frac{1}{T_{T3}} & 0 & 0 & 0 & 0 & 0 & 0 & 0 & 0 \\
0 & \frac{1}{T_{T4}} & 0 & 0 & 0 & 0 & 0 & 0 & 0 \\
0 & 0 & -\frac{apf_1K_1}{T_{G1}} & 0 & 0 & 0 & 0 & 0 & 0 \\
0 & 0 & -\frac{apf_2K_1}{T_{G2}} & 0 & 0 & 0 & 0 & 0 & 0 \\
-\frac{1}{T_{G3}} & 0 & 0 & -\frac{apf_3K_2}{T_{G3}} & 0 & 0 & 0 & 0 & 0 \\
0 & -\frac{1}{T_{G4}} & 0 & -\frac{apf_3K_2}{T_{G3}} & 0 & 0 & 0 & 0 & 0 \\
0 & 0 & 0 & 0 & 1 & 0 & 0 & 0 & 0 \\
0 & 0 & 0 & 0 & -1 & 0 & 0 & 0 & 0 \\
0 & 0 & 0 & 0 & 0 & 0 & 0 & 0 & 0 \\
0 & 0 & 0 & 0 & -\frac{K_{pss}}{2H} & -\frac{1}{T_w} & 0 & 0 & 0 \\
0 & 0 & 0 & 0 & -\frac{K_{pss}T_1}{T_2 2H} & 0 & 0 & 0 & \\
0 & 0 & 0 & 0 & g3 & 0 & 0 & h3 & 0 \\
0 & 0 & 0 & 0 & g4 & 0 & 0 & h4 & -\frac{1}{T_2}
\end{bmatrix}_{25\times25} \tag{6.28}$$

Where,

$x = \begin{bmatrix} \Delta\omega_1 \Delta\omega_2 \Delta\delta_1 \Delta\delta_2 \Delta E'_{q1} \Delta E'_{q2} \Delta E'_{d1} \Delta E'_{d2} \Delta E_{fd1} \Delta E_{fd2} \end{bmatrix}'$ *Contd...*

$x = \begin{bmatrix} \Delta P_{GV1} \Delta P_{GV2} \ \Delta P_{GV3} \Delta P_{GV4} \Delta P_{M1} \Delta P_{M2} \Delta P_{M3} \Delta P_{M4} \end{bmatrix}'$ *Contd...*

$x = \begin{bmatrix} \int ACE_1 dt \int ACE_1 dt \Delta P_{tie1-2} \Delta v_1 \Delta \dot{V}_{pss1} \Delta v_2 \Delta \dot{V}_{pss2} \end{bmatrix}'_{25\times1}$

6.4.2 Design of Ancillary controllers using GA

The multiple PSSs and tie-line power flow TCSC controllers have been designed using real coded genetic algorithm. The different parameters of PSSs and TCSC have been optimized for two area power system. Design of PSSs and TCSC are described as follow :

6.4.2.1 GA based Multiple PSS : Problem Formulation and Optimization Function

The power system stabilizer has been used for frequency stabilization in both area of power system. The rotor speed deviation of area 1 and area 2 have been chosen as input signal for PSS1 and PSS2 proposed controller. The equation (2.5) consists wash out filter time constant T_w, gain K_{pss} and time constant of phase compensator T_1, T_2, T_3 and T_4. Here one stage phase compensator has been used for PSS1 and PSS2. Thus, four parameters such as gain K_{pss1} of PSS1 and K_{pss2} of PSS2, and time constant parameter of phase compensator T_1, T_2, are required to be optimized for the optimal design of both PSS. For both PSS, the time constant of wash out filter T_w has been selected to be 10. The objective of LFC with multiple area PSS is, to reduce the oscillatory frequency in rotor mode and also to minimize the tie line power oscillation in both control area. The goal can be achieved after minimizing the optimization function J, which is described by equation (6.29). The optimization function has been developed such that the damping factor of rotor mode in LFC be improved and minimization of real part of the eigen values associated with same mode. Hence time response parameters such as settling time to be improved and overshoots to be reduced. The Time Multiplied by Absolute Error (ITAE) has been used as the performance index. The optimization function J follows the optimized performance of PSSs controlled system. The gains for the PSSs are adjusted such that the performance index be minimized. The performance index is calculated over a time interval T, normally in the region where t is the settling time of the system. The best system response is obtained when PSSs parameters are optimized and minimizing the maximum real part of eigen values over a

certain range of operating conditions. The optimization flow chart for implementation of real coded GA is similar as shown in Figure 3.1. Only optimization parameters are different, which are described by equations (6.30) to (6.33). The optimization function J is described by following equation (6.29) :

$$J = \int_0^T t(|\Delta\omega_{m1}(t)| + |\Delta\omega_{m2}(t)|)dt \tag{6.29}$$

with

$$K_{pss1}^{min} \leq K_{pss1} \leq K_{pss1}^{max} \tag{6.30}$$

$$K_{pss2}^{min} \leq K_{pss2} \leq K_{pss2}^{max} \tag{6.31}$$

$$T_1^{min} \leq T_1 \leq T_1^{max} \tag{6.32}$$

$$T_2^{min} \leq T_2 \leq T_2^{max} \tag{6.33}$$

6.4.2.2 GA based PSSs and TCSC : Problem Formulation and Optimization Function

The stability loop equation of TCSC (2.89) has been used for frequency stabilization. The input signal rotor speed deviation of area 1 or area 2 has been chosen for TCSC proposed controller. The equation (6.16) consists wash out filter time constant T_{w1}, gain K_{TCSC} and time constant of phase compensator T_{1T}, T_{2T}, T_{3T} and T_{4T}, which provides appropriate phase-lead characteristics to compensate for the phase lag between input and output signals. Five parameters such as gain K_{TCSC} and time constant parameter $T_{1T}, T_{2T}, T_{3T}, T_{4T}$ are required to be optimized for the optimal design of TCSC frequency controller. Four parameters such as gain K_{pss1} of PSS1 and K_{pss2} of PSS2, and time constant parameter of phase compensator T_1, T_2, are required to be optimized for the optimal design of both PSS. For PSSs and TCSC, the time constant of wash out filter has been selected to be 10. The optimization function

described by equation (6.34) has been used for PSSs and TCSC parameters with following constraint as follows :

$$J = \int_0^T t(|\Delta\omega_{m1}(t)| + |\Delta\omega_{m2}(t)|\, dt \tag{6.34}$$

$$T_{1T}^{min} \leq T_{1T} \leq T_{1T}^{max} \tag{6.35}$$

$$T_{2T}^{min} \leq T_{2T} \leq T_{2T}^{max} \tag{6.36}$$

$$T_{3T}^{min} \leq T_{3T} \leq T_{4T}^{max} \tag{6.37}$$

$$T_{4T}^{min} \leq T_{4T} \leq T_{4T}^{max} \tag{6.38}$$

$$K_{TCSC}^{min} \leq K_{TCSC} \leq K_{TCSC}^{max} \tag{6.39}$$

$$K_{pss1}^{min} \leq K_{pss1} \leq K_{pss1}^{max} \tag{6.40}$$

$$K_{pss2}^{min} \leq K_{pss2} \leq K_{pss2}^{max} \tag{6.41}$$

$$T_1^{min} \leq T_1 \leq T_1^{max} \tag{6.42}$$

$$T_2^{min} \leq T_2 \leq T_2^{max} \tag{6.43}$$

6.4.3 Design of Ancillary controllers using ANFIS

The multiple PSSs and tie-line power flow TCSC controllers have been designed using Adaptive Neur-Fuzzy Inference System. The PSSs and TCSC have been designed for two area power system. Design of PSSs and TCSC are described as follow :

6.4.3.1 ANFIS based Multiple PSS

In this work, GA based CPSSs are replaced by the ANFIS based PSSs. The Adaptive Neuro-Fuzzy Inference System based PSS has been developed and tested extensively in chapter 4. The model of ANFIS described in section (4.3.1) has been utilized as PSS1 and PSS2 in two area power system model. The inputs are speed $\Delta\omega_m(t)$ and change in speed $(\frac{\Delta d\omega_m(t)}{dt})$ and corresponding ΔV_{pss} has been selected as output value for the ANFIS1 and ANFIS2 in two area power system model in restructured environment.

6.4.3.2 ANFIS based PSSs and TCSC

In this work, GA based TCSC is replaced by the ANFIS based TCSC. The Adaptive Neuro-Fuzzy Inference System based tie line TCSC has been developed and tested extensively in Chapter 4. The model of ANFIS described in section (4.3.2) has been utilized as TCSC tie line controller. The inputs are speed $\Delta\omega_{m1}(t)$ and change in speed $(\frac{\Delta d\omega_{m1}(t)}{dt})$ and corresponding ΔX_{TCSC} has been selected as output value for the ANFIS controller in two area power system model in restructured environment.

6.4.4 Analysis

The linearized model presented by Figure 6.13 has been used for the stability analysis of the two area system without ancillary controllers and with multiple area PSS and tie line TCSC controller. The first and third operating conditions and corresponding values of machine constant K_1 to K_{10} as shown in Table 3.2 are used for stability analysis of two area power system. For two operating conditions, the oscillations of the electromechanical modes of the machine are identified with PSSs and TCSC and stability of the system has been analyzed. The optimized parameters of PSSs are tuned for expected solution which is given by Table 6.6. Here eigen values and damping factors associated with electromechanical mode are mentioned. eigen values and corresponding damping factor without PSS and with GA based

PSSs are shown in Table 6.7 and Table 6.8 respectively. The optimized parameters of TCSC have been utilized from Table 3.12. eigen values and corresponding damping factor with GA based TCSC and simultaneous application of PSSs and TCSC are shown in Table 6.9 and Table 6.10 respectively.

Table 6.6: Optimized Parameters of PSSs

	Operating Conditions	
Parameters	1	2
K_{pss1}	2.568	4.56
K_{pss2}	2.280	2.69
T_1	0.97	1.83
T_2	0.994	2.419

Table 6.7: Eigen values without PSSs

O.C.	Area 1		Area 2	
	eigen values	ζ	eigen values	ζ
1	0.0030 + 6.4053i	-0.005	0.0038 + 6.4237i	-0.006
	0.0030 - 6.4053i		0.0038 - 6.4237i	
2	0.1370 + 6.8954i	-0.0199	0.1365 + 6.8784i	-0.0198
	0.1370 - 6.8954i		0.1365 - 6.8784i	

Table 6.8: Eigen values with PSSs

O.C.	Area 1		Area 2	
	eigen values	ζ	eigen values	ζ
1	-2.8617 + 6.7807i	0.3888	-2.8629 + 6.7592i	0.3900
	-2.8617 - 6.7807i		-2.8629 - 6.7592i	
2	-3.2075 + 7.4701i	0.3945	-3.2085 + 7.4488i	0.3956
	-3.2075 - 7.4701i		-3.2085 - 7.4488i	

Table 6.9: Eigen values with TCSC

O.C.	Area 1		Area 2	
	eigen values	ζ	eigen values	ζ
1	-3.7524 + 7.5030i	0.4473	0.0017 + 6.4058i	-0.0003
	-3.7524 - 7.5030i		0.0017 - 6.4058i	
2	-7.1835 +11.9598i	0.5149	0.1354 + 6.8788i	-0.0197
	-7.1835 -11.9598i		0.1354 - 6.8788i	

Table 6.10: Eigen values with PSSs and TCSC

O.C.	Area 1		Area 2	
	eigen values	ζ	eigen values	ζ
1	-10.2311 +10.4023i	0.7012	-2.8552 + 6.7546i	0.3893
	-10.2311 -10.4023i		-2.8552 - 6.7546i	
2	-10.1058 +19.1186i	0.4673	-3.2050 + 7.4454i	0.3954
	-10.1058 -19.1186i		-3.2050 - 7.4454i	

The participation factor method has been used for identification of eigen values and damping factors associated to electromechanical mode using TCSC, PSSs and PSSs-TCSC. With only TCSC as shwon in Table 6.9, for the two operating conditions the eigen values associated with area 1 are negative and damping factors are positive, while with area 2, the eigen values and damping factor are positive and negative respectively. Hence eigen values show that only tie line power controller does't provide stability to multi area power system. Attention to Table (6.8), multiple area PSSs improved the eigen values, damping factor and reduced oscillatory frequency in rotor mode of area 1 and area 2. As shown in Table (6.10), the eigen value and damping factor are improved compared to individual application of PSSs and TCSC. So, simultaneous application of PSSs and TCSC have significantly enhanced stability of the system. The closed poles are very far away in the left half of the s-plane using ancillary controllers PSSs-TCSC compared to individual controllers.

6.4.5 Non Linear Simulation

Here, nonlinear simulation has been performed under consideration of normal operating condition and heavy loading operating condition of power system. Here various DPM has been considered with variation of load in control area 1 and area 2. A two area system is used to demonstrate the behavior of the AGC scheme with multiple power system stabilizer and TCSC tie line power controller. The different cases [32] are considered according to the bilateral contract between GENCOs and DISCOs in restructured market. The comparison analysis between GA based PSSs and ANFIS based PSSs in restructured AGC scheme have

been carried out. The performance of simultaneous application of PSSs and TCSC have also been verified. The data described by Appendix A and Appendix B are used for the simulation purpose. The governor and turbine units in each area are assumed to be identical.

Case I :

In this case, the GENCOs in each area participate equally in AGC. ACE participation factors are $apf_1 = 0.5, apf_2 = 0.5, apf_3 = 0.5, apf_4 = 0.5$. Assume that the load change occurs only in area 1. Thus, the load is demanded only by DISCO1 and DISCO2. Load variation in area 1 is $\Delta P_{L1} = 0.05$ p.u., $\Delta P_2 = 0.05$ p.u., $\Delta P_{L1,LOC} = 0.1$p.u. are considered and no disturbances occur in area II. The optimal integral gain $K_1 = 0.9$ and $K_2 = 0.1$ are selected [76]. For this case, the DPM is described by equation (6.44).

For the normal operating condition, speed deviation in area 1 and area 2 has been observed in Figure 6.14. Figure 6.15, 6.16 and 6.17 show individual application of GA and ANFIS based PSSs, and simultaneous application of intelligent based ancillary controllers, which provided good damping characteristics for speed deviation as well as change in tie line power.

The response of speed deviation without ancillary controllers under heavy loading condition has been shown in Figure 6.18. System lost its stability very quickly at 4 second, which shows instability of two area system. The response of speed deviation with GA and ANFIS based PSSs has been shown in Figure 6.19 and 6.20. The response of tie line power changes in both area with TCSC has been shown in Figure 6.21. Responses show that simultaneous application of controllers reduce oscillation in both area and provide stability to system.

$$DPM = \begin{bmatrix} 0.5 & 0.5 & 0 & 0 \\ 0.5 & 0.5 & 0 & 0 \\ 0 & 0 & 0 & 0 \\ 0 & 0 & 0 & 0 \end{bmatrix} \tag{6.44}$$

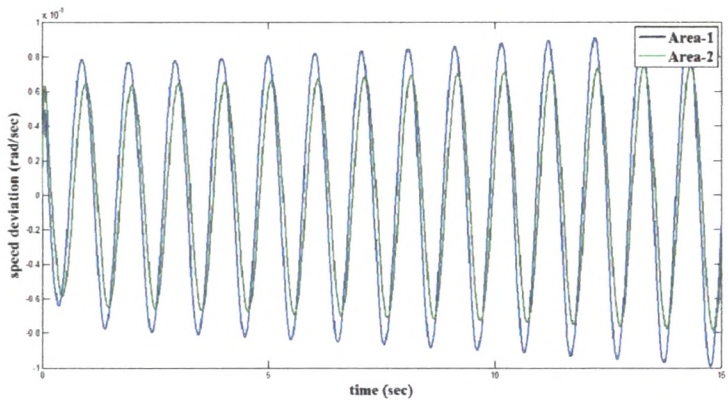

Figure 6.14: Case I: First O.C. : Response of speed deviation in Area 1 and Area 2

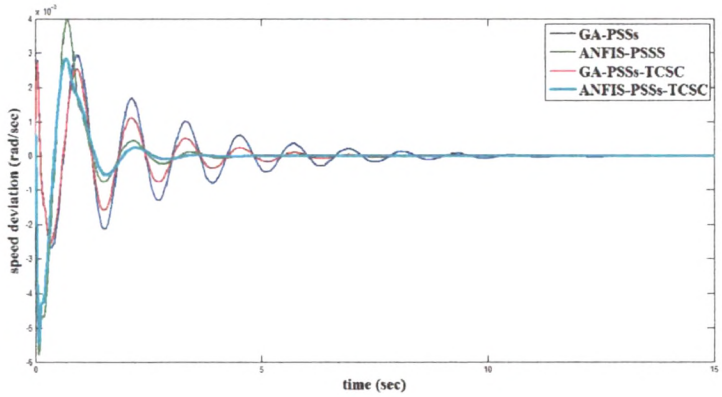

Figure 6.15: Case I : First O.C.: Response of speed deviation in Area 1 with Multiple PSS and TCSC

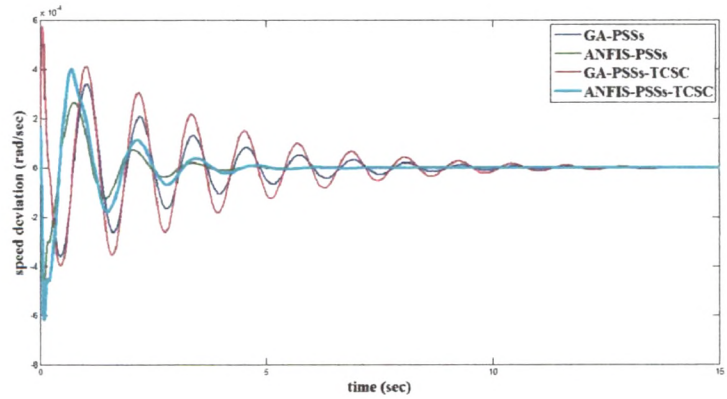

Figure 6.16: Case I: First O.C.: Response of speed deviation in Area 2 with Multiple PSS and TCSC

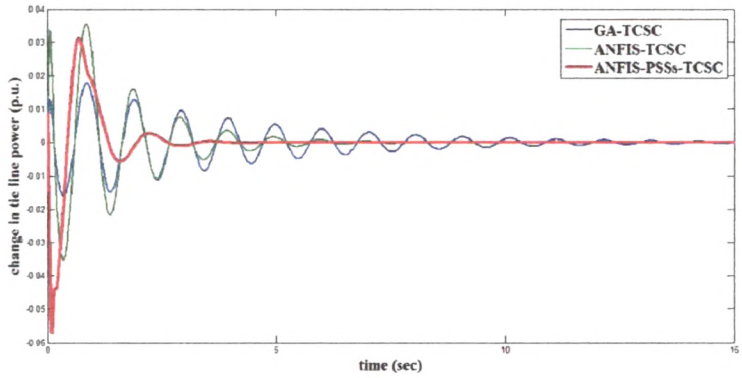

Figure 6.17: Case I: First O.C.: Change in Tie Line Power with Controllers

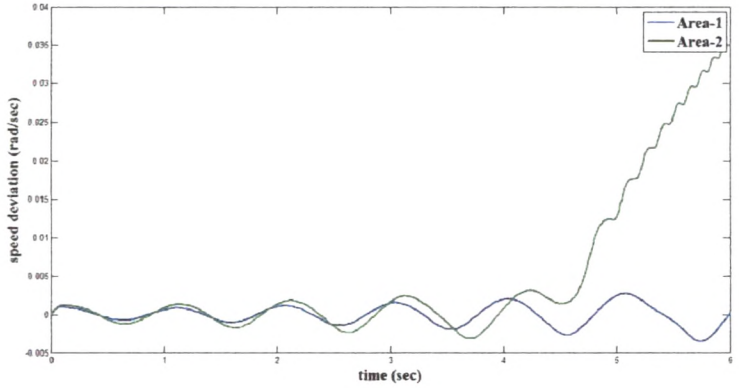

Figure 6.18: Case I: Second O.C.: Response of speed deviation in Area 1 and Area 2

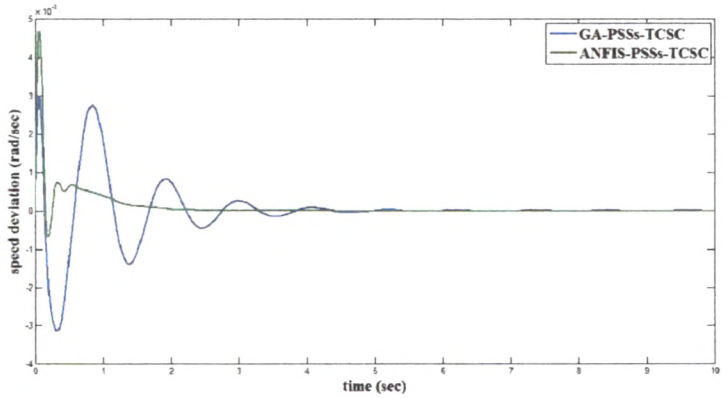

Figure 6.19: Case I: Second O.C.: Response of speed deviation in Area 1 with Multiple PSS and TCSC

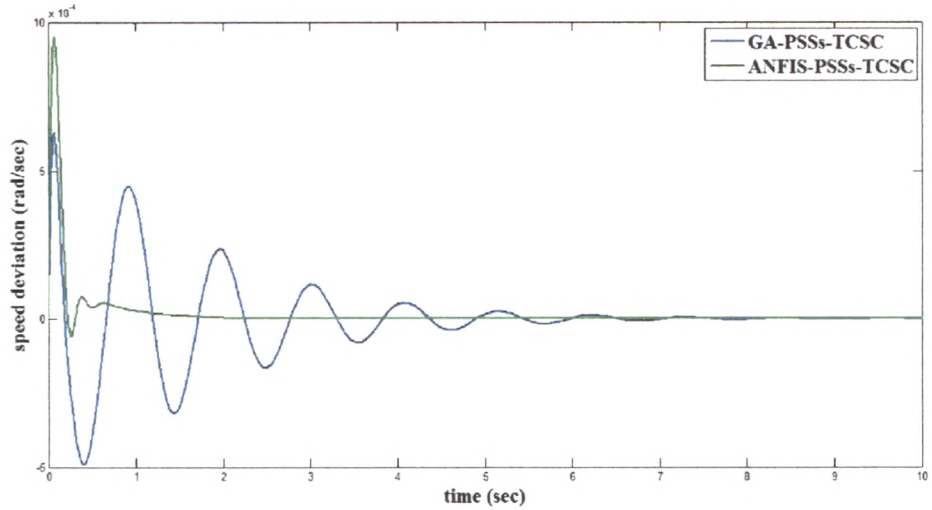

Figure 6.20: Case I: Second O.C.: Response of speed deviation in Area 2 with Multiple PSS and TCSC

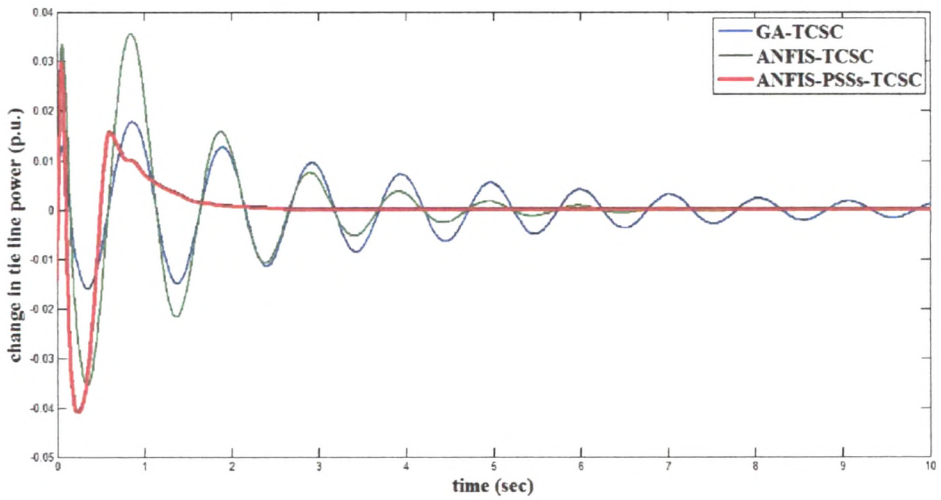

Figure 6.21: Case I: Second O. C.: Change in Tie Line Power with Controllers

Case II:

In this case, where all the DISCOs contract with GENCOs for power as per DPM described by equation (6.45). ACE participation factors are $apf_1 = 0.5, apf_2 = 0.5, apf_3 = 0.5, apf_4 = 0.5$. The load variation are considered such as $\Delta P_{L1} = 0.01$ p.u., $\Delta P_2 = 0.02$ p.u.,$\Delta P_{L3} = -0.05$p.u.,$\Delta P_{L4} = 0.1$p.u.,$\Delta P_{L1,Loc} = -0.1$p.u. and $\Delta P_{L2,Loc} = 0$. For the normal operating condition, speed deviation in area 1 and area 2 has been observed as

shown in Figure 6.22. Figure 6.22 shows that system become unstable and lost stability at 10 second under consideration of DPM described by equation (6.45) and variation of load in control area. Figure 6.23, 6.24 and 6.25 show individual application of PSSs and TCSC, and simultaneous application of intelligent techniques based ancillary controllers, which shows that ancillary controller has provided good damping characteristics for speed deviation as well as change in tie line power.

Under heavy loading conditions, different DPM and variation of load in control area, system comes under unstable mode very fast, which has been shown in Figure 6.18. The response of speed deviation in both area has been shown in Figure 6.27 and 6.28. Change in tie line power in both area with TCSC controller has been shown in Figure 6.29. Figures 6.27, 6.28 and 6.29 show that simultaneous application of intelligent techniques based controllers reduce oscillation in both area and provide stability to system.

$$DPM = \begin{bmatrix} 0.50 & 0.25 & 0.00 & 0.30 \\ 0.20 & 0.25 & 0.00 & 0.00 \\ 0.00 & 0.25 & 1.00 & 0.70 \\ 0.30 & 0.25 & 0.00 & 0.00 \end{bmatrix} \tag{6.45}$$

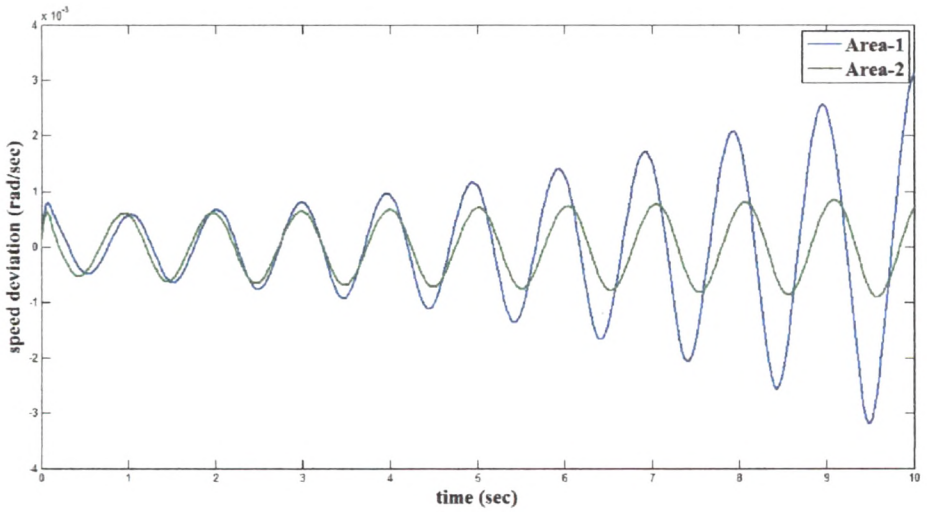

Figure 6.22: Case II: First O.C.: Response of Apeed deviation in Area 1 and Area 2

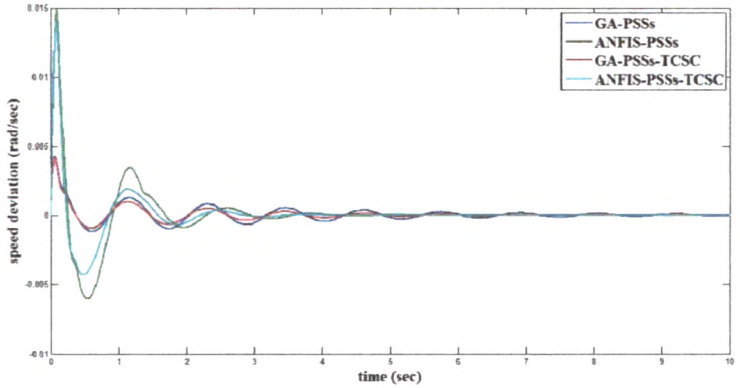

Figure 6.23: Case II: First O.C.: Response of Apeed deviation in Area 1 with Multiple PSS and TCSC

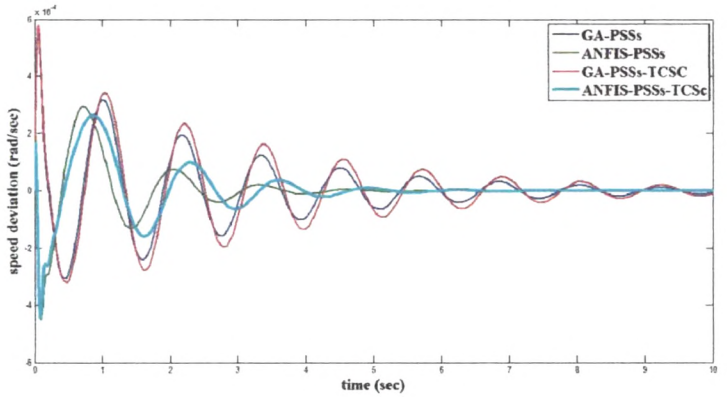

Figure 6.24: Case II: First O.C.: Response of Speed deviation in Area 2 with Multiple PSS and TCSC

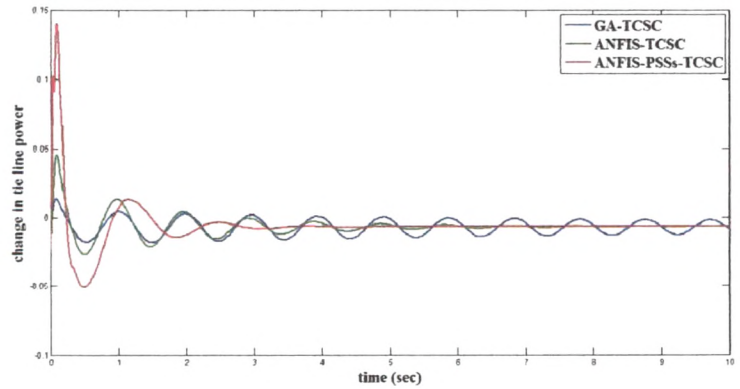

Figure 6.25: Case II: First O.C.: Change in Tie Line Power with Controllers

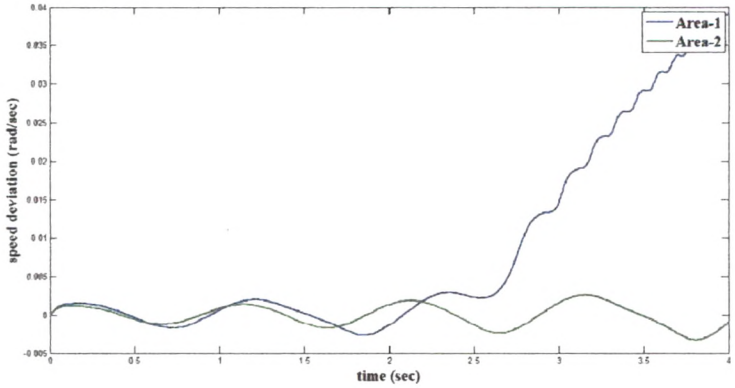

Figure 6.26: Case II: Second O.C.: Response of Speed deviation in Area 1 and Area 2

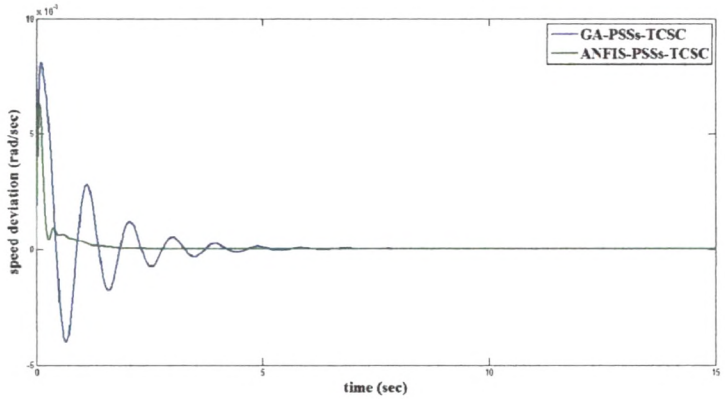

Figure 6.27: Case II: Second O.C.: Response of Speed deviation in Area 1 with Multiple PSS and TCSC

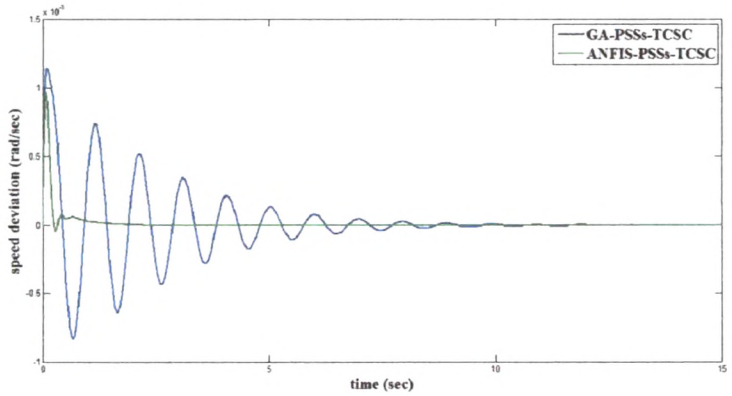

Figure 6.28: Case II: Second O.C.: Response of speed deviation in Area 2 with Multiple PSS and TCSC

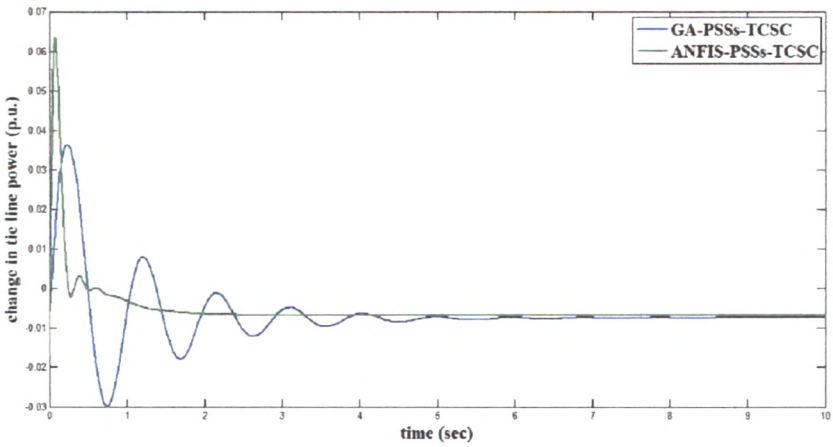

Figure 6.29: Case II: Second O.C.: Change in Tie Line Power with Controllers

6.5 Conclusion

In this study, performance and role of ancillary controllers such as PSS and TCSC have been analyzed in two area control system under restructured electric market. Low order power system model and higher order power system model have been considered for depth analysis of two area system with ancillary controllers. The small signal stability analysis and non-linear simulation for the transient stability analysis have been carried out for investigation of the power system stability issue. Two different operating conditions are taken with consideration of various DPM and load variation in both control area. The rotor speed deviation and change in tie line power have been analyzed under different types of DPM and variation of load in control area.

From first order power system model :

It has been shown that the eigen values associated to the electromechanical mode are more negative with presence of TCSC in two area system and poles in s-plane are far away from origin as shown in Table 6.1. The damping factor has been improved with TCSC compared to that without TCSC, which shows that the LFC system is more stable and TCSC has been provided good damping to oscillation in power system. The effect of various DPM and variation of load have been clearly observed in the simulation results of speed deviation and

change in tie line power. The simulation results have shown that the frequency oscillation and tie line power oscillation have been controlled through GA and ANFIS based TCSC in two area system. The ANFIS based TCSC has been reduced oscillation in speed deviation and tie line power compared to the GA based TCSC. The time response parameters such as settling time and overshoot have been improved using ANFIS based TCSC compared to the GA based TCSC in both control area.

From higher order power system model :

1. GA and ANFIS based control strategies have been developed for designing of multiple PSS and TCSC damping controller. The multiple PSS and simultaneous designed TCSC and PSS have been applied to the dynamical two area power system.

2. It has been shown that the eigen values associated to the electromechanical mode are more negative with presence of multiple PSS and TCSC in multi area power system and poles in s-plane are far away from origin. The damping factor has been improved with PSSs compared to that without PSSs, which has shown that the system is more stable and PSSs have provided good damping to oscillation in power system. It has also been observed that the with simultaneous application of multiple PSS and TCSC in power system, the eigen values are more negative and damping factor has been improved significantly, which shows good stability of system compared to the individual application of PSS and TCSC.

3. From the non - linear analysis, without the application of the controllers in the system, the oscillations in rotor speed deviation and tie line power have been observed. Under the heavy loading conditions in restructured environment, the oscillation in speed deviation are continuously growing which creates the instability of the restructured electric system. Simultaneously designed TCSC and PSS damping controller have significantly diminished oscillations in system. Simultaneous application of TCSC and PSS have provided very good damping characteristics compared to the individual application of PSSs or TCSC and almost eliminate the oscillations in system. Application of ANFIS

based TCSC and PSSs have improved the time response parameters such as settling time, rise time and delay time appreciably and also decreased the overshoot in the system compared to the GA based ancillary controllers.